Desalination and Water Treatment
www.deswater.com

doi: 10.1080/19443994.2014.979448

57 (2016) 2195–2202
January

Taylor & Francis
Taylor & Francis Group

Effects of KOH activation on surface area, porosity and desalination performance of coconut carbon electrodes

Bilal Khalid[a], Qinghan Meng[b,*], Raheel Akram[a], Bing Cao[a,*]

[a]*College of Materials Science and Engineering, Beijing University of Chemical Technology, Beijing 100029, China, Tel. +86 1064432118; email: bcao@mail.buct.edu.cn (B. Cao)*
[b]*The Key Laboratory of Beijing City on Preparation and Processing of Novel Polymer Materials, Beijing University of Chemical Technology, Beijing 100029, China, Tel. +86 1064436876; email: qhmeng@mail.buct.edu.cn*

Received 24 April 2014; Accepted 17 October 2014

ABSTRACT

Coconut carbon was activated by various concentrations of KOH to obtain carbon with different surface area and porosity, hence co-relate the effects of activation on surface area, pore size, and desalination performances of resulted activated carbons. For activation purpose, 0.05, 0.1, 0.2, and 0.5 M KOH solutions were used, subsequently followed by carbonization under N_2 atmosphere. The resulted surface areas were found to be 909.21, 703.47, 647.32, and 601.14 $m^2\ g^{-1}$, respectively. Activated carbon electrodes were prepared with poly tetrafluoroethylene and carbon black, tested for electrosorption of NaCl under 1.6 V. Highest adsorption values were found to be 21, 15, 16, and 26 $mg\ L^{-1}\ g^{-1}$ for 0.05, 0.1, 0.2, and 0.5 M KOH Ac. Brunauer–Emmett–Teller and scanning electron microscopy confirmed the electrodes were porous, and the average pore size was in the range of 2.46–2.81 nm. Furthermore, Fourier transforms infrared spectroscopy spectra were used to investigate the presence of oxygen containing functional groups. The electrical double layer formation was characterized by using cyclic voltammetry.

Keywords: KOH activation; Surface area; Porous carbon; Desalination; Electrical double layer

1. Introduction

Activated carbon is the one of the most commonly used industrial adsorbent and can easily be prepared by physical or chemical activation from different source materials such as coconut shells, wood, peat, and coal. The activation of these materials can generate a carbon material with a developed porous structure and a large specific surface area more than 400 $m^2\ g^{-1}$, but often reach to a value of 1,000 $m^2\ g^{-1}$ [1–3]. However, activated carbon with controlled pore size and pore distribution is highly desirable in many industrial applications. Pore texture, structure, size, and surface area of the finally pyrolysis activated carbon are greatly dependent on both, nature of precursor and activation process.

Activation processes are mainly categorized into two categories for the preparation of activated carbon [4,5] i.e. physical and chemical activation. Physical activation usually involves the carbonization of precursor followed by the gasification of the resulting char or direct CO_2/steam activation of the starting material. Such activation is resulted in most reactive carbon structure atoms generating the porosity. In

---

*Corresponding authors.

contrast to physical activation, chemical activation involves the impregnation of the given precursor with activation agent, after that is pyrolysis. Pyrolysis resulted in higher carbon content with more ordered structure and much developed porosity. Previously reported chemical agents are phosphoric acid, zinc chloride, and alkaline metal compounds [6–8]. Previously, phosphoric acid and zinc chloride have been reported for the activation of lignocellulosic materials [9,10]. However, alkaline-based agents like KOH have been used for coal precursors and chars [11–13]. Literature shows that there is a growing interest in the use of metal hydroxide chemical activating agent like KOH in the production of activated carbon. The main advantages of chemical activations are it needs lower temperature and shorter time as compared with physical activation. Moreover, the yield of the final sample is much higher due to the dehydrogenation properties of chemical agents which inhibits the formation of tar and reduce the production of other volatile substances. The only disadvantage of chemical activation is the washing steps because of the incorporation of the impurities from activating agent, which may affect the chemical properties of the activated carbon. However, such problems can be minimized by using high purity analytical grade activating agents [14]. By considering the importance of chemical activation with its short time process and effective results on final product, we selected it as our activation rout for the activation of coconut carbon.

Due to the low cost, frequent, and effective use of KOH, we decided to use it for the activation of coconut carbon. In this work, we used different strengths of KOH for the activation of coconut carbon. In our work, we studied the effects of concentrations of KOH on the surface area, pore size, structure, and desalination performance of the resulted activated carbon. For the first time, it is observed that specific surface area is decreased with an increase in KOH concentration but the desalination performance is enhanced with this decrease. Secondly, KOH activation has successfully imparted oxygen containing functional groups on the surface, which created some additional attractive force for the ions during electrosorption. It means KOH has created some additional attractive sites in the form of functional groups for ions interactions. For this reason, there are the important factors which are discussed below and are well supported by experimental data of Fourier transforms infrared spectroscopy (FTIR), Brunauer–Emmett–Teller (BET) specific surface area essay, scanning electron microscopy (SEM), cyclic voltammetry (CV), and electrosorption tests of NaCl.

2. Material and method

2.1. HNO_3 treatment

Coconut carbon used in this study was purchased from XINSEN CARBON INDUSTRY CO., LTD FUJIAN. To reduce its ash content, activated carbon was firstly treated with 12 M HNO_3. The resulting material was washed for several times with hot water to remove the acid completely. Acid free carbon was dried at 80°C in an oven for one night.

2.2. KOH activation and carbonization

0.05, 0.1, 0.2, and 0.5 solutions of KOH were prepared in 40 ml of deionized water. Twelve grams of acid-treated carbon was added to each solution and stirred for one hour. After one hour, all solutions were filtered and dried in an oven at 80°C. Dried samples were saved in separate bags for further use. All four samples were placed in a horizontal furnace and heated up to a carbonization temperature of 750°C at a heating rate of 10°C min^{-1} for one hour under N_2 gas flow. After carbonization, the temperature of the furnace was cooled down to the room temperature under N_2 gas flow.

2.3. Electrode preparation

Activated carbon was washed with deionized to remove the KOH. After drying, all samples were grounded to a fine powder and passed through a sieve of 0.076 mm mesh size separately.

Active carbon: Carbon Black: PTFE

80% : 15% : 5%

Activated carbon was mixed with carbon black and 10% solution of ploytetrafluoroethylene (PTFE) binder along with ethanol according to the above composition, the resulted sticky paste was rolled within a circle of 5 cm over nickel foam having 8 cm diameter. two pieces were prepared as cathodes while one piece was prepared from both sides, acted as an anode, dried at 80°C in an oven for one night. These electrodes were used to prepare the cell for the adsorption of various strengths of NaCl electrolyte.

2.4. BET analysis and surface morphology

Specific surface area, pore size distribution of all four samples, and starting material were measured by

BET and BJH methods under N_2 adsorption–desorption method at −77 K on a sorptomatic 1990 Thermo Fisher Scientific Inc analyzer. The surface morphology and structure of pores were characterized by SEM (HITACHI S-4700).

2.5. Fourier transforms infrared spectroscopy

FTIR of activated carbon samples and starting material was carried out by preparing their KBr disks. Each activated carbon sample was mixed with analytical grade of KBr powder. The pellets of 1 mm thickness were prepared by pressing in an electronics hydraulic press. FTIR spectra were recorded under vacuum from 400 to 4,000 cm^{-1} using NICOLET 6700 FTIR THERMO SPECIFIC. About 60 scans were performed with a resolution of 1 cm^{-1} to get the suitable spectra for each sample.

2.6. Electrochemical measurements

The electrochemical properties of Ac electrodes and starting material were done by using CV (CHI.660C SHANGHAI CH INSTRUMENT Co. LTD) in a three electrode cell system of Hg/HgCl as a reference electrode and a Pt rod as a counter electrode with 0.01 M NaCl solution. CV measurements were done with a scan rate of 50 mv s^{-1} with an applied voltage of −1 to 1. All electrochemical experiments were carried out at room temperature.

3. Results and discussion

In this study, the coconut carbon was treated with 12 M HNO_3 to reduce its ash content and improve its conductivity. This treatment created a lot of small pores on the surface of carbon which were due to the evolvement of NO_2, CO_2, and some other gases. The resulting material's ash content was found to be 0.65%.

3.1. KOH activation and BET surface area

For activation, we used the different strengths of KOH which were 0.05, 0.1, 0.2, and 0.5. The as reported reaction between KOH and carbon in the furnace shows the formation of solid K_2CO_3 [15].

$$6KOH + C \rightarrow 2K + 3H_2 + 2K_2CO_3$$

The above reaction is thermodynamically favorable at 750°C. In our experiments, it is shown that the surface area and the pore size are greatly affected by the formation of K_2CO_3. Table 1 shows that the surface area decreased as the concentration of KOH increased. This decrease in surface area was due to the formation of solid K_2CO_3.

This suggested that probably activation temperature was not enough to decompose the K_2CO_3 by the evolvement of CO and CO_2. Despite of decomposition, alkaline metal carbonates were melted and penetrated into initially developed pores, hence blocked and caused a decrease in surface area. Molten K_2CO_3 also affected the pore size and their structure as well. Literature shows KOH treatment resulted in the formation of different functional groups i.e. hydroxyl group, carbonyl group, and carboxyl group on the surface of active carbons [16]. These groups are hydrophilic in nature and it is well known that hydrophilic functional groups such as carboxyl and hydroxyl enhance adsorption of inorganic ions in solution by ion-exchange reaction. Such an effect is evident in our electrosorption experiments. Acid treatment resulted in the emission of brown gas. The as proposed chemical reaction between C and HNO_3 is as follow.

$$C + 4HNO_3 \rightarrow 4NO_{2(g)} + CO_{2(g)} + 2H_2O$$

This acid treatment built some micro pores on the carbon surface as it is found in Fig. 2(a). In order to get carbon with different surface areas and porosity, the acid treated starting material was treated with four different concentrations of KOH. Both Table 1 and Fig. 1 shows the surface areas, pore volume, pore size, and BJH pore size distribution of all carbon samples including starting material. BET analysis also indicated a decrease in surface area with increasing KOH concentration. Formation of alkali metal carbonates of KOH and their subsequent conversion to K_2CO_3 was the key factor of this decrease.

Starting material having the surface area of 567.70 $m^2 g^{-1}$ while the 0.05 M KOH Ac has 909.21 $m^2 g^{-1}$. This indicates that lowest concentration of KOH yielded Ac with highest surface area due to the less formation of K_2CO_3. Increased KOH concentration led to an increased production of K_2CO_3, which penetrated into carbon surface and lower the porosity. Another reason for decrease in surface area was the incorporation of smaller pores into the pores of larger diameter or the accumulation of one bigger pore on the surface of many smaller pores. As the activation temperature was little lower than that of the boiling point of KOH, hence KOH melted and entered into the interior of initially developed pores resulting in a poor outer activation with smaller pore size. Fig. 2 shows N_2 adsorption–desorption for all samples and starting material, which exhibited type I isotherm

Table 1
Results of BET surface areas and pore size information

Samples	BET surface area ($m^2 g^{-1}$)	Total pore volume ($cm^3 g^{-1}$)	Average pore size (nm)
Starting material	567.70	0.40	2.81
0.05 M KOH A	909.21	0.58	2.55
0.1 M KOH Ac	703.47	0.48	2.72
0.2 M KOH Ac	647.32	0.37	2.46
0.5 M KOH Ac	601.14	0.39	2.59

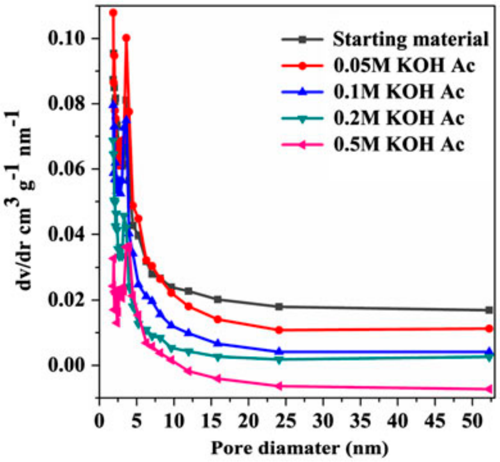

Fig. 1. BJH pore size distributions.

indicated the presence of micro pores as well few mesopores.

3.2. Surface morphologies

Fig. 3 shows the SEM images of both activated carbons samples and starting material. The pores of staring material resulted after HNO_3 are looking uniform and of small size. In our experiments, it was observed that the concentration of KOH greatly influenced the pores size and their shapes. Lower concentration of KOH resulted in small K_2CO_3 formation which blocked only few pores. However, as the concentration increased many of smaller pores combined together to give a new pore whose inner diameter is smaller as its opening diameter, this resulted in an irregular pore distribution with irregular shape. The decrease in surface area with an increase in KOH concentration was due to this factor. SEM images show that some of the pores have undergone in size reduction therefore became even smaller, while many others have been completely blocked resulting in flat surface during activation process.

3.3. FTIR analysis

FTIR spectrums of all Ac samples along with starting material are shown in Fig. 4. HNO_3 treatment resulted in the formation of function groups on the surface of Ac. The band at 3,430 cm^{-1} corresponds to –OH stretching of hydroxyl group, which is presented in all Ac samples and starting material. The peaks at 1,048 and 1,741 cm^{-1} correspond to C=O and C–O stretching vibrations of COOH groups. The peaks at 1,365 and 1,630 cm^{-1} are associated with C–OH and O–H bending vibrations. These two peaks are not much stronger in case of 0.05 and 0.1 M KOH Ac probably it is due to low concentration of KOH. Another reason may also be possible, which is the decomposition of these groups into CO during activation. However, in case of 0.2 and 0.5 M KOH Ac, the concentration was very high which hindered the decomposition process, ultimately saved a reasonable amount of functional groups. These groups were observed with their characteristics peaks in Fig. 6.

3.4. Cyclic voltammetry studies

The CV results for all Ac samples and starting material are presented in Fig. 5. The cyclic voltammograms were taken without any Faradaic reaction, pH change, and bubble formation. Cyclic voltammetry behavior presented a formation of electrical double-layer between carbon electrodes and the ions of electrolyte. All the electrodes displayed a capacitive charging current in both scanning directions across the potential range −1 to +1 V with 0.01 M NaCl. The cyclic voltammograms for all electrodes were taken at a scan rate of 50 mv s^{-1}. Fig. 5 shows that all electrodes can form electrical double layers under charge potential, when charge potential reversed, formed EDLs gradually diminished. The cyclic voltammograms of starting material having different shape and peak as compared to Ac electrodes this is due to the difference in surface area and the presence of oxygen containing functional groups. Because KOH treatment

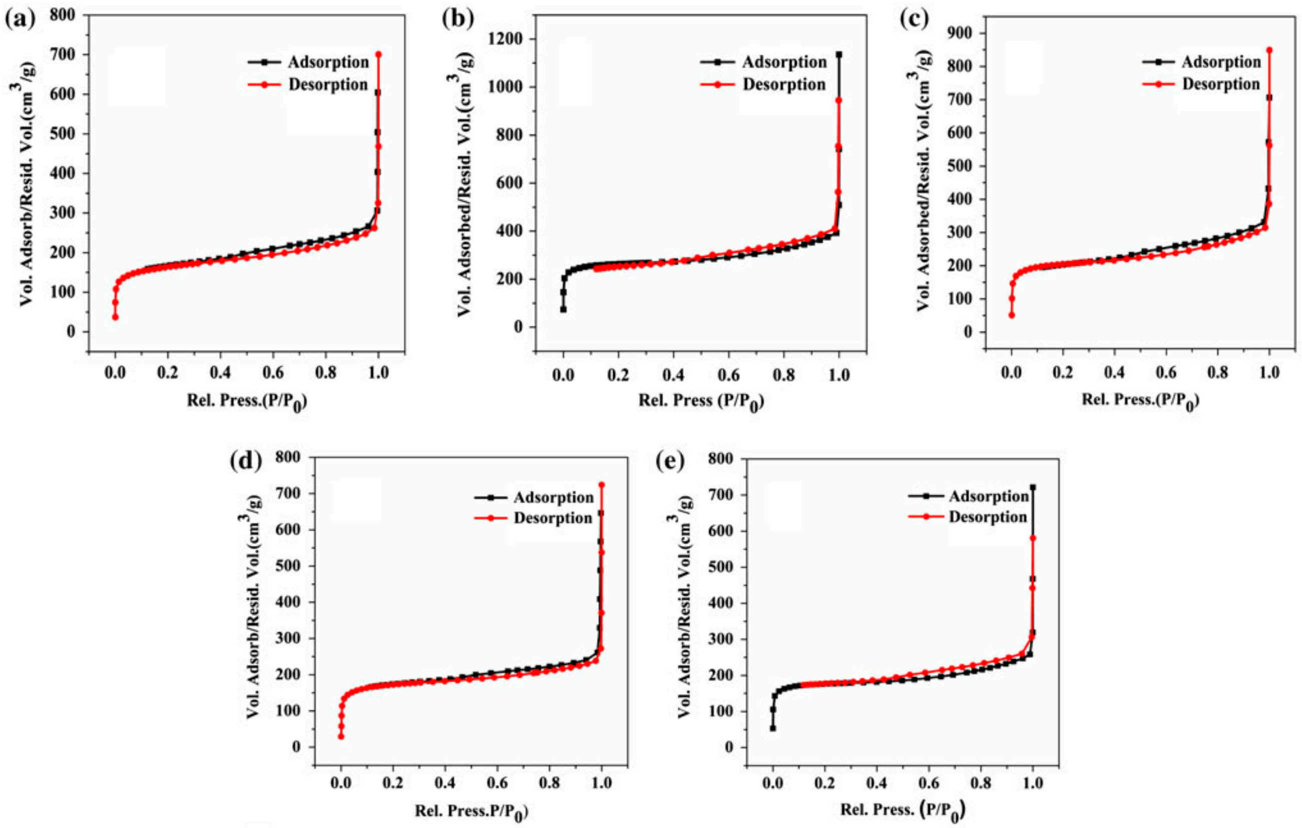

Fig. 2. N_2 adsorption–desorption isotherms (a) starting material, (b) 0.05 M KOH Ac, (c) 0.1 M KOH Ac, (d) 0.2 M KOH Ac, and (e) 0.5 M KOH Ac.

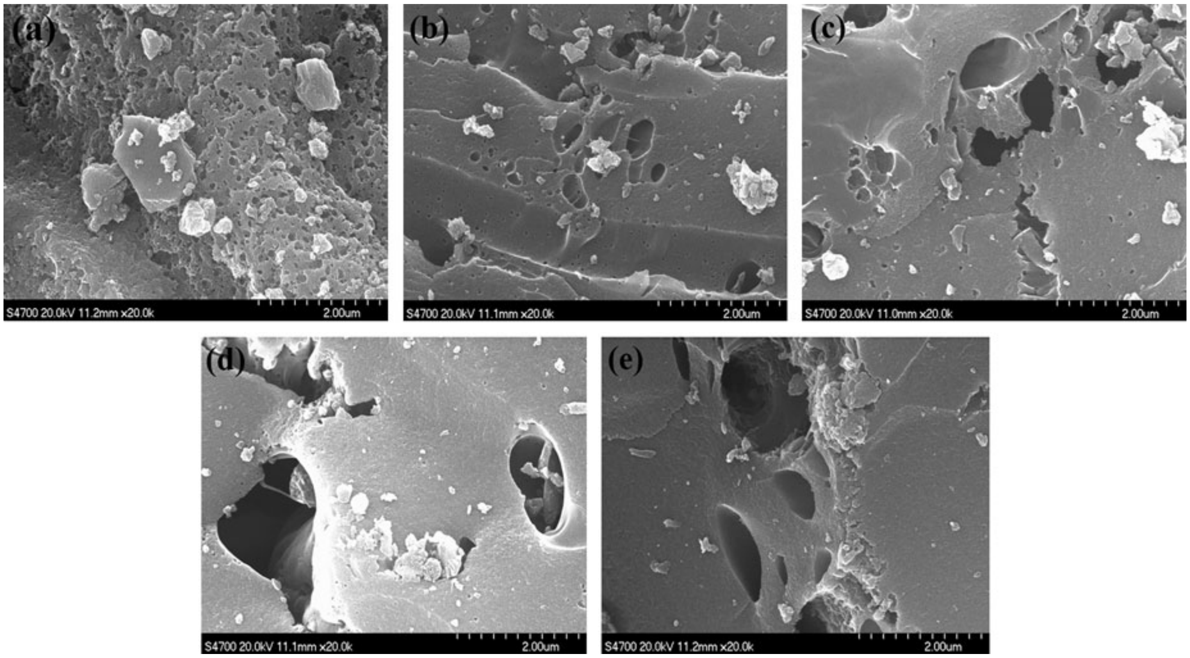

Fig. 3. SEM images (a) starting material, (b) 0.05 M KOH Ac, (c) 0.1 M KOH Ac, (d) 0.2 M KOH Ac, and (e) 0.5 M KOH Ac.

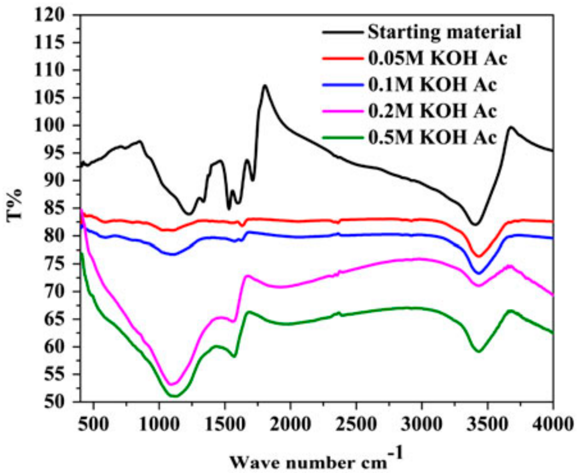

Fig. 4. FTIR spectra of starting material and activated carbon with 0.05, 0.1, 0.2, 0.5 M KOH solutions.

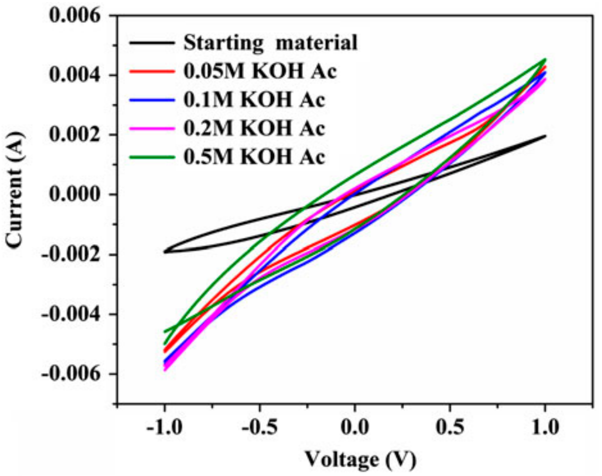

Fig. 5. Cyclic voltammograms for starting material and KOH-activated carbon samples.

could change the functional groups on the surface of pore structure. Fig. 5 shows the increased peaks of cyclic voltammograms for KOH-activated carbon electrodes as compared to untreated starting material. It is reported that the presence of hydrophilic functional groups such as carboxyl and hydroxyl enhance adsorption of inorganic ions in solution by ion-exchange reaction. It was reported [17] that KOH treatment led to a percentage increase in functional groups, as a result, the electrochemical behavior of KOH-activated electrodes was affected by the characteristics of both hydroxyl and carbonyl functional groups. This might be due to weak faradaic reaction other than EDLs process. However, in case of 0.05 M KOH Ac, increase in capacitance is due to surface area, whereas in case of 0.5 M KOH Ac pseudo-capacitive effect of functional groups is the dominant factor. Capacitances of 0.1 M KOH Ac and 0.2 M KOH Ac are nearly equal, whereas there is a big difference in their surface areas. It is suggested the presence of more functional groups in case of 0.2 M KOH Ac is the dominant factor in closeness of the capacitance value.

3.5. Electrosorption performance

The adsorption values comparison for all four Ac electrodes is shown in Fig. 6. The pore size of all Ac electrodes calculated by N_2 adsorption according to BJH method was found to be larger than the size of N_2 molecule, mainly, 0.36 nm [18]. This value is approximately very close to 0.361 nm that is the size of Cl^- ion. These values indicate that Cl^- ions can even penetrate into the pores of all Ac electrodes. Since, Ac used in all four electrodes in this work was derived from same starting material so it was expected that Ac with larger surface area would have strong electrical double-layers EDLs formation. However, in our electrosorption experiments, it was observed that adsorption of NaCl was not linearly proportional to the surface area. Fig. 6 shows that 0.5 M KOH Ac having highest adsorption of NaCl with lowest surface area. While 0.05 M KOH Ac with highest surface area also showed some comparable

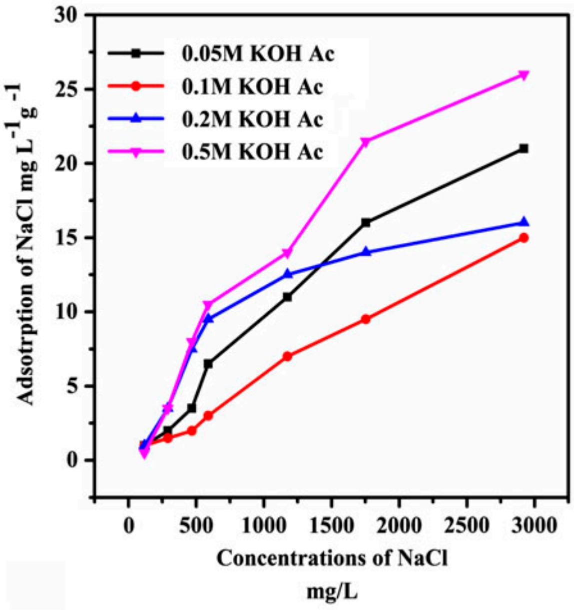

Fig. 6. A comparison of adsorption values of activated carbon samples.

adsorption rate at higher initial concentration of NaCl electrolyte. Table 1 shows that the average pore size of these two Ac is of approximately same size but the structures and the shapes of pores are very different. In case of 0.05 M KOH Ac and 0.5 M KOH Ac, the increase in adsorption rate was rapid with increase in NaCl concentrations. Whereas, this type of increase in case of 0.1 M KOH Ac and 0.2 M KOH Ac was very smooth and low from one lower concentration to next higher concentration.

This type of mechanism was due to the irregularity of pore structure which can be seen from SEM image in Fig. 3. While the pore structure in case of 0.05 M KOH Ac is looking proper so can leads to a better EDLs formation. It was observed that all four Ac electrodes had shown almost similar adsorption with low concentrations of NaCl. The main reason for this was the excess of microporosity and improper pore structure in all four Ac electrodes, which was responsible for weaker EDLs formation at lower concentrations of NaCl. Secondly, at such lower concentrations Na^+ and Cl^- ions could not reside in the pores for a long time even though the applied voltage was 1.6 V. The improper porous structure led to weaker EDLs. However, as the concentration was increased the adsorption also increased to considerable amount. For this reason, it can be thought as the charge on the surface of the electrodes was increased the electrostatic attraction was also increased. This led to the formation of some stronger EDLs even with smaller surface area and improper pore size. This type of phenomenon was not found with lower concentrations because there was less charge which was not enough for the formation of stronger EDLs. Also, there were the chances of collapsing of EDLs in case of lower concentrations. Same collapsing of EDLs could also be happened in higher concentration, but due to enhanced charge density it was compensated. Here, the role of surface functional groups present on carbon surface created by KOH activation could not be ignored. KOH treatment created a lot of functional groups such as carboxyl, carbonyl, hydroxyl, and phenol. These functional groups could play an important role in adsorption mechanism. These oxygen containing groups enhanced the adsorption rate by attracting the respective ions in the electrolyte. The unusual behavior of 0.5 M KOH Ac electrode might be due to this reason. The effect of these functional groups could not be neglected in case of other three electrodes but due to better pore size, higher surface area it was not so prominent there. Adsorption mechanism in all four KOH Ac was purely surface adsorption phenomenon along with electrostatic interactions between applied voltages and ions, as it involved the pores and surface for the accumulation of ions under the influence of applied voltages, so it is categorized as surface adsorption phenomenon.

4. Conclusion

Different concentrations of KOH were used to prepare the activated carbons of coconut shell. Modification of coconut carbon with KOH and its effects on BET surface area, porosity, and adsorption of NaCl were studied. Different concentrations of KOH produced activated carbon with different porosity and surface area. It was cleared from electrosorption and CV measurements that KOH resulted in the formation of functional groups which played their role in adsorption. KOH activation has given a variety of function groups on the pore's structure, which enhanced adsorption for inorganic ions. This study has provided an understanding of KOH activation and its effects on desalination performance regarding surface area and porosity. This is beneficial for the production of activated carbon electrodes for desalination industry.

References

[1] J.W. Shim, S.M. Lee, B.S. Rhee, S.K. Ryu, Adsorption of Ni(II), Cu(II), Cr(VI) from multicomponent aqueous solution by pitch-based ACF, in: Extended Abstracts, European Carbon Conference, Newcastle, UK, British Carbon Group, 1996, pp. 242–243.
[2] F. Rodríguez-reinoso, The role of carbon materials in heterogeneous catalysis, Carbon 36 (1998) 159–175.
[3] L.H. Peebles Jr., Carbon nanofibers, in: R. Vajtai (Ed.), Carbon Fibers: Formation, Structure, and Properties, CRC, Ann Arbor, MI, 1995, pp. 125–155.
[4] R.C. Bansal, J.B. Donnet, F. Stoeckli, Active Carbon, Marcel Dekker, New York, NY, 1988.
[5] Roskill. The Economics Of Activated Carbon, Roskill Information Services Ltd, London, 1990.
[6] A. Ahmadpour, D.D. Duong, Preparation of activated carbons from Spanish anthracite: I activation by KOH, Carbon 34 (1996) 471–479.
[7] M.J.B. Evans, E. Halliop, J.A.F. MacDonald, The production of chemically-activated carbon, Carbon 37 (1999) 269–274.
[8] A. Ahmadpour, A.K. Bradley, D.D. Do, Comparison of equilibria and kinetics of high surface area activated carbon produced from different precursors and by different chemical treatments, Ind. Eng. Chem. Res. 37 (1998) 1329–1334.
[9] F. Caturla, M. Molina-Sabio, F. Rodríguez-Reinoso, Preparation of activated carbon by chemical activation with $ZnCl_2$, Carbon 29 (1991) 999–1007.
[10] F. Rodr´ıguez-Reinoso, M. Molina-SabioM, Activated carbons from lignocellulosic materials by chemical and/or physical activation: An overview, Carbon 30 (1992) 1111–1118.

[11] M.J. Illán-Gómez, A. García-García, C. Salinas-Martínez de Lecea, A. Linares-Solano, Activated carbons from Spanish coals. 2: Chemical activation, Energy Fuels 10 (1996) 1108–1114.

[12] H. Teng, T.S. Yeh, L.Y. Hsu, Preparation of activated carbon from bituminous coal with phosphoric acid activation, Carbon 36 (1998) 1387–1395.

[13] A. Ahmadpour, D.D. Do, The preparation of activated carbon from macadamia nutshell by chemical activation, Carbon 35 (1997) 1723–1732.

[14] Z. Zhu, A. Li, L. Yan, F. Liu, Q. Zhang, Preparation and characterization of highly mesoporous spherical activated carbons from divinylbenzene-derived polymer by $ZnCl_2$ activation, J. Colloid Interface Sci. 316 (2007) 628–634.

[15] M.A. Lillo-Ródenas, D. Cazorla-Amorós, A. Linares-Solano, Understanding chemical reactions between carbons and NaOH and KOH, Carbon 41 (2003) 267–275.

[16] H.J. Oh, J.H. Lee, H.J. Ahn, Y. Jeong, Y.J. Kim, C.S. Chi, Nanoporous activated carbon cloth for capacitive deionization of aqueous solution, Thin Solid Film 515 (2005) 220–225.

[17] J. Koresh, A. Soffer, Study of molecular sieve carbons. Part 2—Estimation of cross-sectional diameters of non-spherical molecules, J. Chem. Soc. Faraday Trans. 1: Phys. Chem Conens. Phases 76 (1980) 2472–2483.

[18] H. Harned, S.S. Owen, Physical Properties of Electrolytic Solution, third ed., Reinhold, New York, NY, 1958.